Nowcasting Applications of a Microwave Radiometer in Hong Kong

P.W. Chan[1]

[1]*Hong Kong Observatory, 134A Nathan Road, Kowloon, Hong Kong, China, pwchan@hko.gov.hk*

ABSTRACT

Trials of ground-based, multi-channel microwave radiometers were conducted in Hong Kong for several months in 2004 and 2006. Following these trials, a permanent unit has been installed in Hong Kong since February 2008. The present paper discusses the performance and nowcasting applications of this instrument during the past year. A number of temperature and humidity retrieval methods have been tried out in the study period and the retrieval method based on linear regression of historical data for the whole year is found to have the best performance in comparison with co-located radiosonde data. The integrated water vapour and liquid water path measurements from the radiometer are found to have generally good correlation with radiosonde and weather radar data respectively. For nowcasting applications, K-index is calculated from the temperature and humidity profiles from the radiometer. It turns out to have good correlation with the integrated water vapour, which could only be studied using the continuous thermodynamic profiles available from the radiometer. Moreover, the average K-index in rain episodes is found to have reasonable correlation with the total number of lightning flashes within about 10-40 km from the radiometer, a proxy of the instability of the atmosphere, similar to the study results of Chan (2009).

1. INTRODUCTION

A ground-based microwave radiometer (model: RPG HATPRO from Radiometer Physics) has been working at the Hong Kong International Airport (HKIA) since May 2008. It uses 14 frequency channels (7 for oxygen and 7 for water vapour) to measure the temperature and the humidity profiles up to 10 km continuously (with data updated every few seconds). Compared with radiosonde ascents that are only launched a couple of times a day, the radiometer enables continuous monitoring of the thermodynamic conditions of the troposphere, which could be useful in the nowcasting of heavy rain and wind gusts associated with intense convective weather. Such applications have been studied in the previous field experiments of radiometers in Hong Kong as documented, e.g. in Chan (2009) for subtropical coastal area.

With the acquisition of a permanent unit, a more comprehensive study of the performance and application of the microwave radiometer could be carried out at HKIA. This paper would firstly examine the performance of the different retrieval algorithms for thermodynamic profiles and the integrated quantities (e.g. integrated water vapour, IWV, and liquid water path, LWP). The use of K index derived from the radiometer data in the nowcasting of intense convective weather would also be studied.

2. RETRIEVAL ALGORITHMS FOR THERMODYNAMIC PROFILES

The radiometer at HKIA gives the temperature and the relative humidity profiles up to 10 km based on regression equations of the raw brightness temperatures at the various frequency channels that are established from climatological radiosonde data. It turns out that such regression equations are not quite robust in situations of rain, even for light rain. In this section, the performance of the various retrieval algorithms for thermodynamic profiles would be studied by excluding rain cases. In the later sections, the radiometer data at times of rain would also be considered and in such situations, the relative humidity profile is assumed to be saturated for simplicity. The retrieval algorithms are found to be much better, especially in rainy weather, using neural network (NN) approach as discussed in Chan (2009). Further studies of the same radiometer dataset but with the use of NN algorithm would be discussed in a separate paper.

The performance of retrieval algorithms is examined during the period when the radiometer was placed at the headquarters of the Hong Kong Observatory (HKO) in downtown Hong Kong, which is situated at about 1 km south of the radiosonde station at King's Park. The period of study is February to April 2008 (i.e. before the relocation of the radiometer to HKIA). A number of regression equations are considered.

For the retrieval of temperature profiles, the methods used include:

(a) Considering only the boundary-layer scans using the oxygen frequency channels for the whole year (All_tpb);

(b) Considering only the zenith scans using the oxygen frequency channels for the whole year (All_tpc); and

(c) Similar to (b), but using a seasonal approach, namely, instead of considering the data over the whole year, only seasonal (3-monthly) data are employed in the establishment of regression equations, i.e. there would be four sets of regression equations for use in the four seasons (3_month_tpc).

The comparison results with radiosonde data (launched three times a day during the study period, namely, 00, 06 and 12 UTC) are shown in Figure 1. It turns out that All_tpc generally performs the best in the

lower troposphere (below 3 km or so) and 3_month_tpc performs better aloft.

There are also several ways of establishing the regression equations for relative humidity profiles. In all cases, only the zenith scans are used. The methods include:

(a) Considering all the 14 frequency channels together in the establishment of the regression equations for the whole year (All_14_hpc);

(b) Similar to (a) but consider the 7 water vapour channels only (All_7_hpc);

(c) Similar to (a) but also consider the surface humidity sensor (All_14SS_hpc);

(d) Similar to (a) but consider the monthly data (i.e. 12 regression equations for a whole year, monthly_hpc); and

(e) Similar to (a) but consider the seasonal data (i.e. 4 regression equations for a whole year, 3_month_hpc).

The performance of the above methods is shown in Figure 2. Probably with the inclusion of the surface sensor, All_14SS_hpc performs the best in the boundary layer, up to about 1,500 m. For higher altitudes, the All_7_hpc generally performs the best.

After considering Figures 1 and 2, it looks like the establishment of regression equations using shorter periods of time (e.g. seasonal) does not seem to have significant advantages over the conventional method of considering the data over the whole year. On the other hand, the inclusion of surface sensor could improve the performance of the retrieval in the lower troposphere. As such, instead of using low-quality ground sensors to give the radiometer users a rough idea about the conditions near the surface, it is recommended to employ well-calibrated ground sensors and include them in the retrieval algorithm of the thermodynamic profiles of the radiometer.

3. INTEGRATED QUANTITIES

IWV from the radiometer is compared against the equivalent quantity, normally called total precipitable water vapour (TPW) from radiosonde. The study period is one whole year, namely, between June 2008 and May 2009. The comparison result is given in Figure 3. It could be seen that the two quantities are well correlated, with a correlation coefficient (R^2) reaching about 0.79. However, there are some data points in which the IWV from the radiometer is too much higher in comparison to the radiosonde data. Similar behaviour was also seen in the previous study (Chan, 2009). The reason for the discrepancy would require further studies.

LWP from the radiometer is compared against the vertically integrated liquid (VIL) from a weather radar in Hong Kong (considering the VIL value at the grid point which is closest to HKIA, with a grid size of about 260 m). The period of study is June to August 2008. Due to the large volume of radar data, only a shorter period is considered here. Nonetheless the study period is the rain season in Hong Kong and the data sample considered should be representative of the typical rainy weather in the region. To the knowledge of the author, this is the first time that such a comparison is made. The two quantities show reasonable correlation (Figure 4), with a correlation coefficient reaching about 0.6. There are a number of observations: (i) in general the LWP from the radiometer is larger, (ii) however, there are some isolated data points in which VIL is larger, and (iii) the LWP value is capped at about 10. The reasons of these observations would be studied further.

4. K INDEX

The K indexes obtained from the radiometer and the radiosonde are compared in Figure 5. The study period is also one year, namely, June 2008 to May 2009. The two datasets are well correlated, with a correlation coefficient reaching about 0.8. The slope is close to unity and the y-intercept is close to 0.

Both K index and IWV from the radiometer could be useful for the nowcasting of intense convective weather. It would be interesting to find out if the two quantities are correlated with each other in the climatic condition in Hong Kong. The two datasets are plotted together with Figure 6. Possibly because the water vapour is mostly concentrated in the lower troposphere, the two quantities are found to have good correlation, especially for drier weather (K index below 20 or so). For more humid weather, it turns out that IWV rises much more rapidly with the increase of K.

Similar to the study in Chan (2009), the correlation between the temporally averaged K index in rain episodes and the degree of convective instability (using number of lightning flashes as a proxy) is studied again. However, due to the large volume of lightning data, only a short period of April to July 2008 is considered in this paper. A longer period would be studied in future papers. The two quantities are found to have reasonable correlation (Figure 7), apart from a few data points in which the temporally averaged K index is large but the number of lightning flashes is much smaller than the best-fit straight line to the dataset. It turns out that these outliners pertain to tropical cyclone cases. Therefore, though rainy weather associated with both surface troughs and tropical cyclones could have large K index values, the lightning behaviour would be rather different.

By not considering the tropical cyclone cases, the correlation coefficient of the best-fit straight line (as shown in Figure 7) for considering lightning flashes within different distances away from the radiometer is plotted in Figure 8. It appears that the radiometer (through the temporally averaged K index) may be representative of the instability of the troposphere within a distance of 10-40 km from the instrument.

5. CONCLUSIONS

In this paper, a number of retrieval algorithms of thermodynamic profiles for the microwave radiometer are considered and the performance of the integrated quantities is established by comparing with similar measurements by independent instruments. The K index is useful for nowcasting intense convective weather and is established for the first time (according to the knowledge of the author) about its correlation

with IWV, at least for the climatic conditions in Hong Kong. As in Chan (2009), the temporally averaged K index is found to have reasonable correlation with the tropospheric instability as revealed by considering the number of lightning flashes within 10-40 km of the radiometer.

REFERENCES

[1] Chan, P.W., 2009: Performance and application of a multi-wavelength, ground-based microwave radiometer in intense convective weather, *Meteorologische Zeitschrift*, **18**, 253-265.

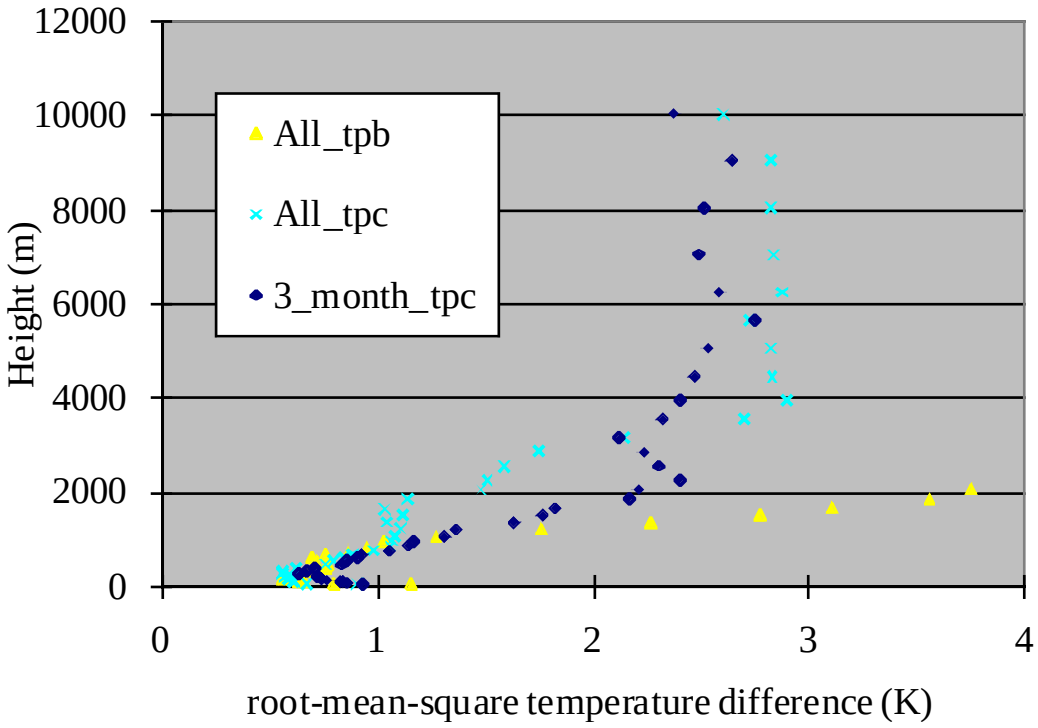

Figure 1 Root-mean-square temperature difference (between radiometer and radiosonde) for different retrieval algorithms for vertical temperature profile of the microwave radiometer.

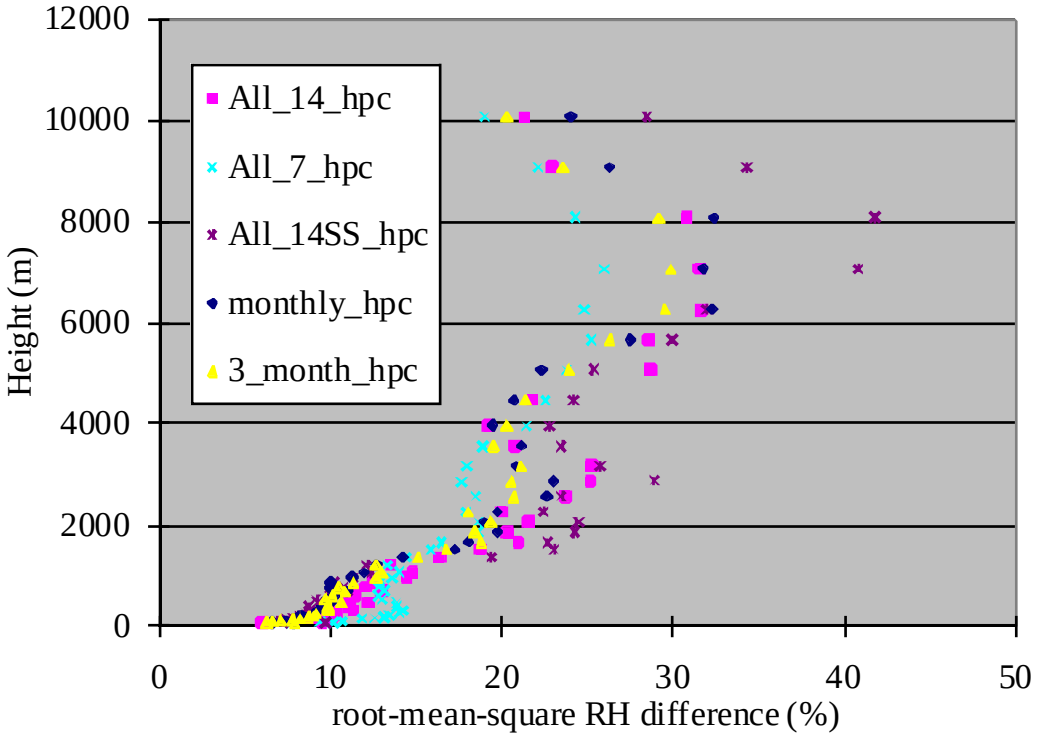

Figure 2 Root-mean-square relative humidity (RH) difference (between radiometer and radisonde) for different retrieval algorithms for vertical RH profile of the microwave radiometer.

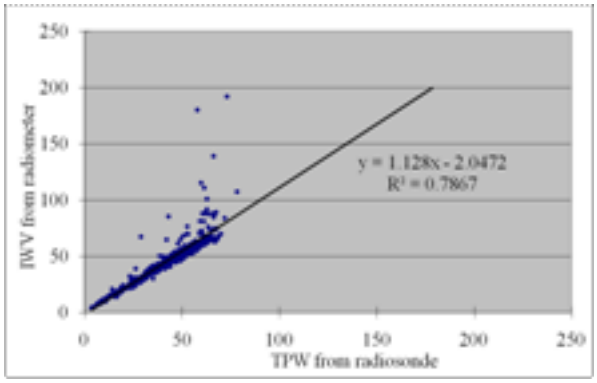

Figure 3 Comparison between IWV of the radiometer and the TPW from the radiosonde at the same time.

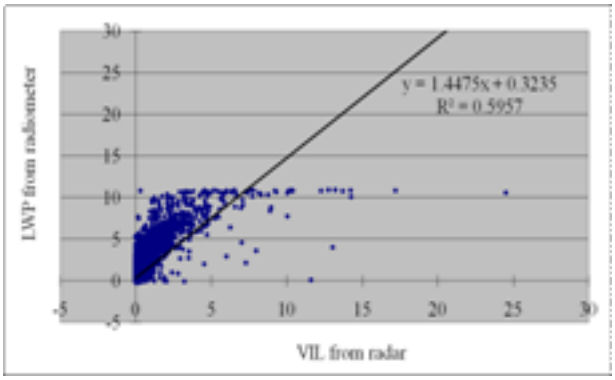

Figure 4 Comparison between LWP from the radiometer and VIL from the microwave weather radar at the same location (HKIA) and same time.

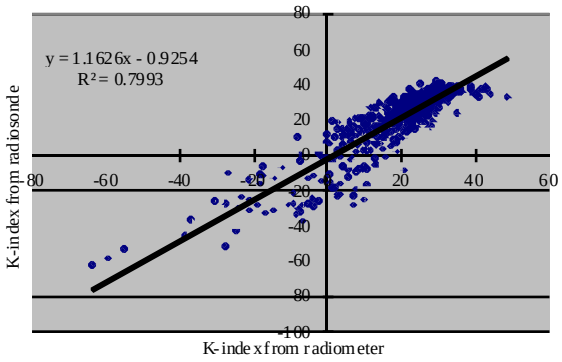

Figure 5 Comparison of K index from the radiometer and the radiosonde at the same time.

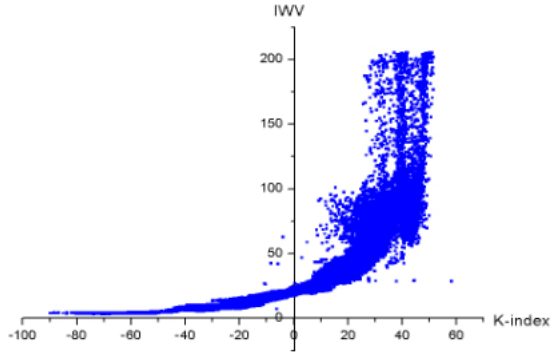

Figure 6 Scatter plot of the K index and IWV as obtained from the radiometer at the same time.

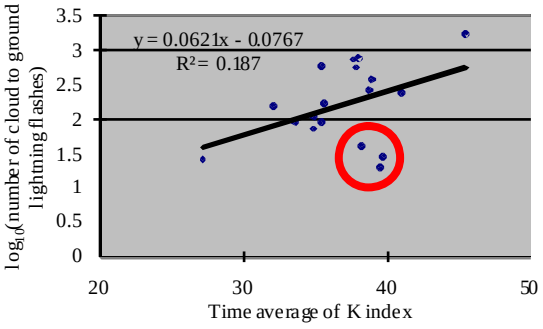

Figure 7 Scatter plot of the temporally averaged K index and the number of cloud-to-ground lightning flashes within 20 km from the radiometer. The data points corresponding to tropical cyclone cases are enclosed in a red ellipse.

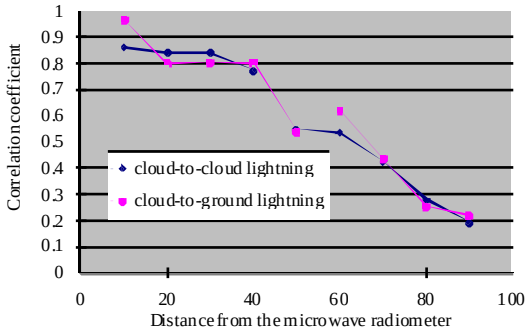

Figure 8 Correlation coefficient (as obtained in graphs similar to Figure 7 but not considering the tropical cyclone cases) as a function of distance from the radiometer (distance within which lightning flashes are counted). Two kinds of lightning are considered, namely, cloud-to-cloud flashes (blue) and cloud-to-ground flashes (pink).